

# Loop Heat Pipe Wick Fabrication via Additive Manufacturing

Bradley Richard<sup>1\*</sup>, Devin Pellicone<sup>1</sup> and William G. Anderson<sup>1</sup>

<sup>1</sup>Advanced Cooling Technologies, Inc., Lancaster, PA, USA

## Abstract

CubeSats and SmallSats are increasing in popularity and capability, but also are requiring improved thermal management to keep up with increasing heat loads and fluxes. Loop heat pipes (LHPs) offer a passive and proven solution, but are currently too expensive for many cost sensitive small satellite projects. By developing 3D printed LHPs using a direct metal laser sintering (DMLS) process the fabrication costs can significantly be reduced while offering increased reliability with the elimination of the knife-edge seal. An optimization study was completed on DMLS parameters for 316LSS to minimize the pore size of 3D printed primary wicks. A minimum pore radius of 5.6 $\mu$ m was achieved. A proof of concept LHP prototype was built with a 3D printed primary wick. Experimental testing was completed. A maximum power of 125W at steady state was achieved. Additionally, low power startup, adverse elevation, and power cycle tests were completed to verify performance over a wide range of conditions. Based on the success of the proof of concept prototype more development is underway for optimization of 3D printed primary wicks, and parameters for secondary wick fabrication.

*Keywords:* Loop heat pipe; Primary wick; Additive manufacturing; CubeSats

## 1. INTRODUCTION

Interest in small satellites is continuing to grow rapidly due to the low costs and short development timelines. There has also been significant progress in the miniaturization of electronics increasing the capabilities of smaller satellites. However, the use of these more powerful electronics require more advanced thermal management systems. Currently, CubeSats and SmallSats primarily rely on the use of high thermal conductivity materials such as graphite and aluminum to spread heat throughout the structure. The use of loop heat pipes (LHPs) would allow for the heat transport over longer distances making deployable radiators possible. The challenge lies in reducing the fabrication costs of LHPs to make their use on cost sensitive small satellites feasible.

Additive manufacturing has the potential to significantly reduce LHP fabrication costs while offering improved reliability. By using 3D printing many steps in the fabrication of LHP evaporators can be eliminated including machining of the wick and wick insertion into the aluminum saddle. Additionally, the wick and fully dense envelope can be made as a single part eliminating the need for a knife-edge seal to prevent back-flow of vapor directly to the compensation chamber. This offers increased reliability as the knife-edge is a bimetallic joint which may fail over long term exposure to thermal cycles and shock and vibration. In this work 3D printing parameters were identified for primary wick

fabrication and a proof of concept prototype LHP was built and tested.

### 1.1 Loop Heat Pipes

LHPs are passive devices capable of high thermal conductances across long distances. A schematic of a LHP is provided in Fig. 1. Heat enters the evaporator and vaporizes the working fluid. The vapor passes through grooves in the primary wick and through the vapor line to the condenser. Here the vapor is condensed and subcooled. The subcooled liquid passes through the bayonet tube into the center of the primary wick. A secondary wick allows for communication between the compensation chamber and center of the primary wick. The compensation chamber contains saturated fluid at a lower pressure than the evaporator which provides the driving force for fluid flow. The capillary pressure of the primary wick must be greater than the total pressure drop of the system to pump liquid from the liquid line return to the evaporation site at the vapor grooves [1].

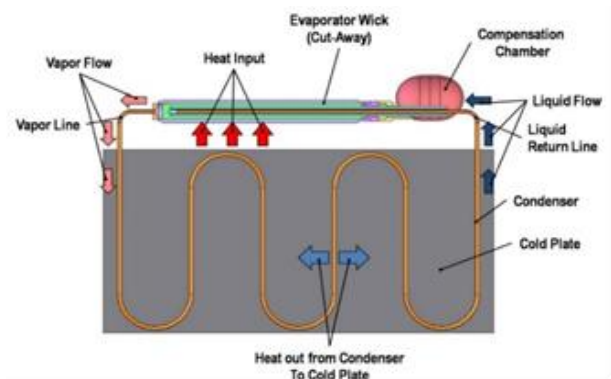


Fig. 1. Loop heat pipe schematic (not to scale).

\*Corresponding author: Bradley.richard@1-act.com, Phone: +1-717-205-0646

## 1.2 3D Printing Wicks

The performance of a LHP primary wick depends largely on pore size. The capillary pressure of a wick is inversely proportional to pore radius. For successful LHP operation the capillary pressure must be greater than the total system pressure drop. Therefore, by reducing the pore size of the primary wick the maximum power can be increased. Traditionally sintered primary wicks have a pore radius of approximately 1  $\mu\text{m}$ . DMLS has been demonstrated to be able of printing porous lattice structures, but the smallest pore size to date has been about 50 $\mu\text{m}$ . This is due to the accuracy and precision of the laser as well as thermal stresses and heat spreading.

In this work a different approach was taken towards 3D printed wick structures. Instead of building a defined lattice structure, the laser power, speed, and spacing was varied to partially sinter the metal powder together instead of fully melting the particles. This results in a wick structure very similar to that of traditionally sintered wicks.

## 2. EXPERIMENTAL SECTION

### 2.1 DMLS Parameter Study

An optimization study was completed on small scale samples to determine the DMLS parameters which resulted in the smallest wick pore size. A total of 15 samples were tested. Each sample had a length of 1in. and a diameter of 0.5in. An EOSINT M280 machine was used for fabrication. Each sample had a different combination of laser power, speed, and spacing. The metal powder used was 316LSS with a diameter of 20 $\mu\text{m}$ .

The pore radius of each sample was measured using the bubble test. One end of the sample was submerged in methanol while the other was attached to a pressurized nitrogen line. The pressure of the nitrogen was slowly increased until bubbles were seen passing through the wick. The pressure at the onset of the first continuous bubble stream was used to calculate the pore radius using Eq. 1

$$R_p = \frac{2\sigma}{P_b} \quad (1)$$

where  $R_p$  is the pore radius,  $\sigma$  is the surface tension of the fluid used, and  $P_b$  is the bubble point pressure.

### 2.2 LHP Prototype

A complete LHP prototype was fabricated for proof of concept testing. Ammonia was used as the working fluid. All wetted parts were 316LSS. The vapor line, condenser line, and liquid line all had a diameter of 0.125in. The condenser was 120in. in length. A picture of the completed LHP prototype is

provided in Fig. 2. The primary wick was 1in. in diameter and 4in. in length. A picture of the primary wick is provided in Fig. 3. The primary wick was printed with a fully dense envelope. This allowed the primary wick to be welded directly to the compensation chamber without the use of a knife-edge seal. Performance testing of the LHP prototype consisted of steady state, low power startup, adverse elevation, and power cycling. The sink temperature for all tests was set to 0 $^{\circ}\text{C}$ .

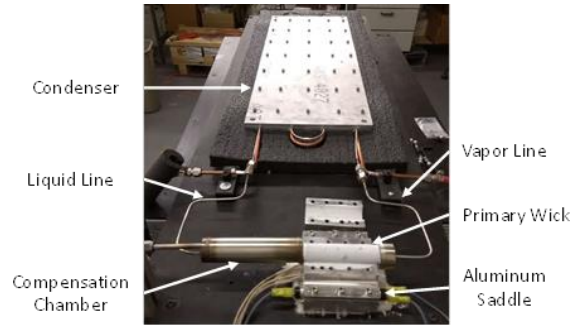


Fig. 2. Completed LHP prototype with 3D printed primary wick.

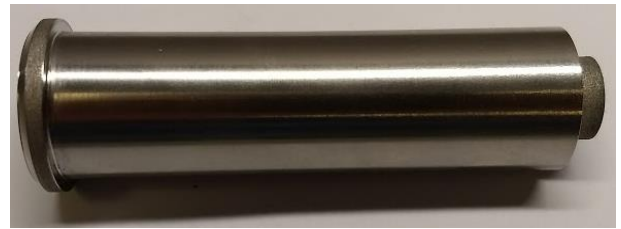


Fig. 3. Primary wick used for proof of concept prototype.

## 3. RESULTS AND DISCUSSION

### 3.1 DMLS Parameter Study

A magnified image of a 3D printed wick sample from the DMLS parameter optimization study is shown in Fig. 4. As expected the appearance is similar to that of traditionally sintered wicks. This is due to using adjusted laser power, speed, and spacing to sinter the 316LSS powder together instead of printing a defined lattice structure. A table comparing the pore radius measured on all 15 samples is presented in Table 1. The samples labeled as hollow did not have sufficient laser power to sinter the metal powder together. The samples labeled as solid had too high of laser power and did not have a continuous porous structure. Sample 2 achieved the smallest pore size with a pore radius of 5.6 $\mu\text{m}$ , and was therefore chosen for use in prototype fabrication and testing. A limit of 5-6 $\mu\text{m}$  for the pore radius was observed with multiple samples approaching that value. This is expected to be a result of using 20 $\mu\text{m}$  diameter 316LSS powder as the build material. Reducing the powder diameter further would allow for small pore sizes to be

achieved, but these are not currently commercially available.

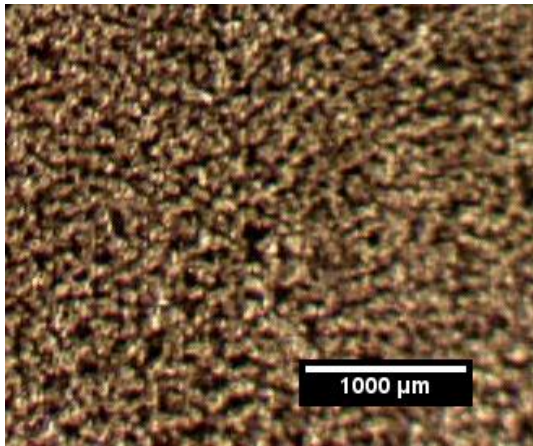


Fig. 4. Image of 3D printed wick structure from DMLS parameter optimization study.

Table 1. Results of DMLS parameter optimization study

Sample	Pore Radius
	μm
1	6.2
2	5.6
3	11.6
4	10.3
5	Hollow
6	Solid
7	Solid
8	Solid
9	6.0
10	8.8
11	Hollow
12	31.4
13	20.0
14	13.7
15	29.9

### 3.2 LHP Prototype

A temperature plot for steady state testing of the LHP prototype with 3D printed primary wick is provided in Fig. 5. Startup occurred immediately after a power of 110W was applied to the evaporator. This is indicated by the rapid drop in liquid line temperature. Once steady state was reached the heat load was increased in 5W increments. Steady state operation was successfully reached at powers of 110, 115, 120, and 125W. When the heat load was further increased to 130W the temperature of the compensation chamber and primary wick continued to rise linearly indicating that dry-out of the primary wick had occurred.

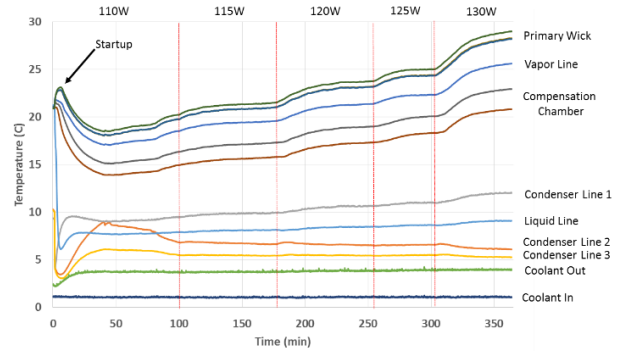


Fig. 5. Steady state testing of LHP prototype demonstrating a maximum operating power of 125W with a sink temperature of 0°C.

A temperature plot of the low power startup test is shown in Fig. 6. A power of 5W was applied to the evaporator. The primary wick slowly heated up until there was sufficient superheating of the liquid ammonia in the vapor grooves to promote boiling. The ability to start the LHP at a power of only 5W indicates that the amount of heat leak is small, because significant heat leak would cause the primary wick and compensation chamber temperatures to increase together preventing LHP operation.

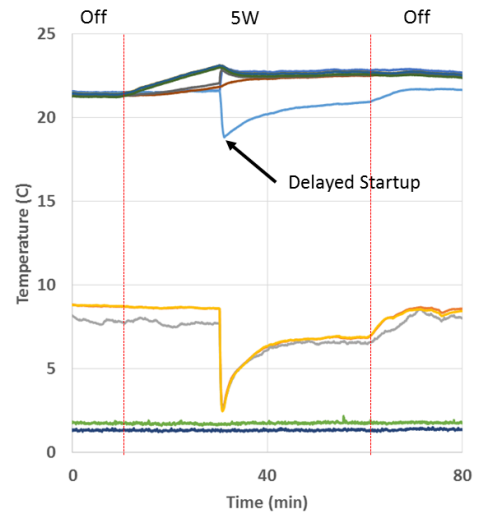


Fig. 6. Successful startup of LHP prototype at a heat input of 5W as indicated by the rapid decrease in liquid line temperature.

Testing was completed with the evaporator raised 6in. above the condenser to verify the ability of the LHP to operate against gravity. A temperature plot of the results is presented in Fig. 7. Startup and steady state operation were successful at powers of 50W and 70W.

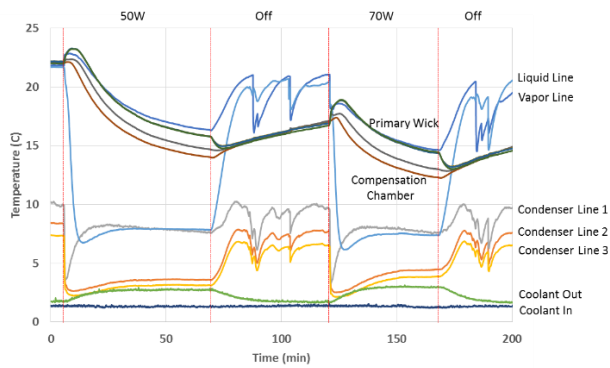


Fig. 7. Test results with 6in. of adverse elevation between the evaporator and condenser. Steady state operation was reached at powers of 50W and 70W.

Power cycle testing was completed to verify the ability of the LHP prototype to handle transients. The power was rapidly changed between 70W and 20W. A temperature plot of the results is shown in Fig. 8. Dry-out did not occur with rapid increases or decreases in power. This indicates that the secondary wick was able to maintain the supply of liquid to the primary wick during transient operation.

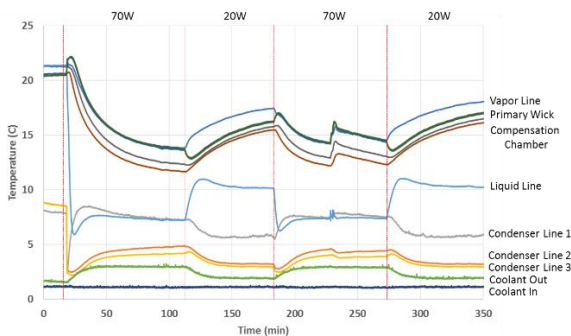


Fig. 8. Rapid power cycling between 70W and 20W test results demonstrating the ability of the secondary wick to prevent primary wick dry-out during transients.

#### 4. CONCLUSIONS

The feasibility of using DMLS for fabrication of LHP evaporators was verified. Through an experimental optimization study, DMLS parameters for producing wicks with a pore radius of 5.6 $\mu$ m were developed. This is sufficient to make LHPs with power levels of 100-200W which is in the range of small satellites. Testing of the prototype LHP with 3D printed primary wick was successful in reaching a maximum power of 125W. The LHP also was able to operate at low powers, against gravity, and survive transients. Therefore, further development is warranted. Next steps include optimization of the primary wick design to increase the maximum power, and development of DMLS parameters for secondary wick fabrication. Once parameters for 3D printing

secondary wicks are developed the entire LHP will be able to be 3D printed. This offers significant cost advantages to traditional LHP fabrication techniques.

#### ACKNOWLEDGEMENT

This work was funded by NASA through the Small Business Innovation Research (SBIR) program.

#### NOMENCLATURE

$P_b$  : Bubble point pressure (Pa)  
 $R_p$  : Pore radius (m)  
 $\sigma$  : Surface tension (N/m)

#### REFERENCES

- [1] Ku, Jentung. Operating characteristics of loop heat pipes. No. 1999-01-2007. SAE Technical Paper, 1999.